Biomacromolecules

ACS AuthorChoice

Article

pubs.acs.org/Biomac

Terms of Use

Cationic PAMAM Dendrimers as Pore-Blocking Binary Toxin Inhibitors

Philip Förstner,[†,‡] Fabienne Bayer,[†,‡] Nnanya Kalu,[§] Susanne Felsen,[‡] Christina Förtsch,[‡] Abrar Aloufi,[§] David Y. W. Ng,[∥] Tanja Weil,[∥] Ekaterina M. Nestorovich,*[,§] and Holger Barth*[,‡]

[‡]Institute of Pharmacology and Toxicology, University of Ulm Medical Center, D-89081 Ulm, Germany

[§]Department of Biology, The Catholic University of America, Washington, D.C. 20064, United States

[∥]Institute of Organic Chemistry III, University of Ulm, D-89081 Ulm, Germany

Supporting Information

ABSTRACT: Dendrimers are unique highly branched macromolecules with numerous groundbreaking biomedical applications under development. Here we identified poly(amido amine) (PAMAM) dendrimers as novel blockers for the pore-forming B components of the binary anthrax toxin (PA_{63}) and *Clostridium botulinum* C2 toxin (C2IIa). These pores are essential for delivery of the enzymatic A components of the internalized toxins from endosomes into the cytosol of target cells. We demonstrate that at low μM concentrations cationic PAMAM dendrimers block PA_{63} and C2IIa to inhibit channel-mediated transport of the A components, thereby protecting HeLa and Vero cells from intoxication. By channel reconstitution and high-resolution current recording, we show that the PAMAM dendrimers obstruct transmembrane PA_{63} and C2IIa pores in planar lipid bilayers at nM concentrations. These findings suggest a new potential role for the PAMAM dendrimers as effective polyvalent channel-blocking inhibitors, which can protect human target cells from intoxication with binary toxins from pathogenic bacteria.

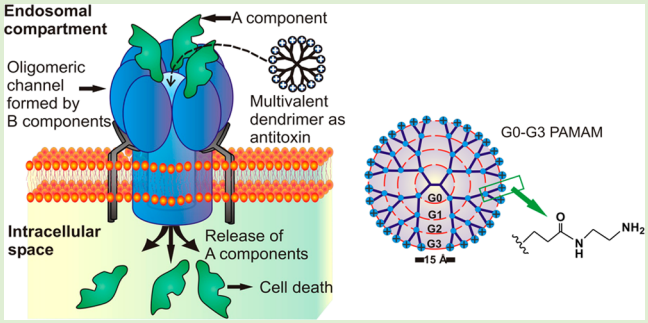

INTRODUCTION

Attaching multiple functional groups onto an inert scaffold is very beneficial for drug design objectives.[1,2] These multiligand compounds often possess an additive or cooperative affinity toward multiple binding sites which is significantly higher than that of a single functional group interacting with a single binding site.[1] Thus, a number of bacterial protein toxins have recently been successfully neutralized by a variety of new synthetic multivalent pharmaceutical agents.[3] Examples include biospecific small-molecule or peptide-based ligands attached to liposome, polymer, or cyclodextrin scaffolds active against anthrax toxins,[4−14] C2 toxin, iota toxin,[15,16] α-hemolysin,[17,18] TcdA, TcdB,[19] cholera toxin,[20−22] heat-labile enterotoxin,[23−25] leukotoxins,[26] shiga toxin,[27−32] and ricin.[33] Some of these multivalent antitoxins were rationally designed with a specific universal target in mind[34] − the ion-conductive transmembrane pores formed by the B components of binary bacterial toxins.[6,15]

Several pathogenic species of *Bacilli* and *Clostridia* secrete clinically relevant binary exotoxins, which consist of two (three in the case of anthrax toxin) individual nonlinked proteins, an enzymatic active A component and a binding/translocation B component.[35,36] Following A/B complex formation on the surface of target cells and subsequent receptor-mediated endocytosis, binary toxins deliver their A moieties from the lumen of acidified endosomes into the cytosol. To this end, the B components insert into endosomal membranes and generate transmembrane pores, which serve as translocation channels for the A components.[35,36] This mechanism is used by anthrax toxin, the major virulence factor of *Bacillus anthracis*, and C2 toxin, an enterotoxin from *Clostridium botulinum*, which are the focus of this study.

The B components of anthrax and C2 toxins, PA (83 kDa) and C2IIa (~80 or ~100 kDa, depending on the strain), correspondingly, are structurally conserved.[35,36] They share high amino acid homology and numerous functional similarities, whereas the A components of these toxins are distinct and target different cell functions.[35,36] The anthrax toxin consists of two A components: lethal factor (LF) and edema factor (EF). In the cytosol, the zinc−metalloprotease LF hydrolyzes mitogen-activated protein kinase kinases (MAPKKs)[37,38] and activates NLRP1,[39] which results in apoptosis of macrophages. EF is a calmodulin-dependent adenylyl cyclase[40] that aids in dissemination of *B. anthracis* in the host.[41] The newly identified key tissue targets responsible for the toxic effects of lethal and edema toxins include two vital

Received: March 3, 2014
Revised: June 13, 2014
Published: June 23, 2014

   dx.doi.org/10.1021/bm500328v | *Biomacromolecules* 2014, 15, 2461−2474

systems, the cardiovascular system (LT) and liver (ET).[42] The A component of clostridial C2 toxin (C2I, ~50 kDa) acts through mono-ADP-ribosylation of G-actin, resulting in F-actin depolymerization, cell rounding and apoptotic cell death.[43−45]

Formation of toxin complexes begins with the binding of PA_{63} and C2IIa to their distinct cellular receptors and the assembly of their A components. Both PA and C2II require proteolytic activation to form the ring-shaped heptameric PA_{63} and C2IIa.[46,47] Activated PA was also reported to form functional octamers.[48] After receptor-mediated endocytosis, PA_{63} and C2IIa change their conformation due to the acidic conditions in the endosomes and insert as ion-permeable, cation-selective pores into the endosomal membranes.[49−51] LF/EF or C2I translocate as partially unfolded proteins through PA_{63} or C2IIa pores, respectively.[52,53] With both PA_{63} and C2IIa, phenylalanine clamps (ϕ-clamp), F427 and F428, respectively, were found to catalyze the unfolding and translocation of the A component across the membrane.[54−58] When inserted into planar bilayer membranes, the PA_{63} and C2IIa channels share similar current noise and voltage gating characteristics.[16] Interestingly, PA_{63} is able to bind and translocate His-tagged C2I, whereas C2IIa does not translocate EF and LF.[59] The similarities suggest that the pore-forming B components could serve as specific universal targets for potential broad-spectrum antitoxins against the *Bacillus* and *Clostridium* pathogenic species.[15,16]

Many tested compounds, which are positively charged at mildly acidic pH, interact with the PA_{63} and C2IIa channel lumens in planar lipid bilayers.[51,54,60−63] In rational design of multivalent toxin inhibitors, once a biospecific ligand is identified (positively charged groups in our system), the next important step is the search for a suitable scaffold to attach the ligands.[64] As a result, synthetic tailor-made cationic 7-positively charged compounds based on a 7-fold symmetrical β-cyclodextrin core were introduced as highly effective, potentially universal blockers of pore-forming subunits of anthrax toxin, C2 toxin, and iota toxin of *C. perfringens* active in vitro, in cells and, in the case of the anthrax toxin, in vivo.[6,10,14,15,65,66]

Here we explore a new group of potential multivalent pore-blocking antitoxins—dendrimers, which are the repeatedly branched polymers with all bonds emanating from a central core. We focus on commercially available cationic PAMAM dendrimers, which are based on an ethylene diamine core and an amidoamine repeat branching structure (Supporting Information, Figure S1). In contrast to traditional linear polymers, dendrimers can be tuned by controllable branched chemical syntheses.[67] As a result, they possess the unique properties: nanosize range, monodispersity, and rigid and stable globular structure with a large and well-regulated number of functional groups and surface charges.[67] Among various industrial and medical applications, dendrimers were investigated as antimicrobial, antiviral and antiparasitic agents.[68] Bacterial toxin-inhibiting properties of the dendrimers were also reported.[33,69−71] Dendrimer-related studies on ion channels are limited. Thus, Howorka's group engineered dendrimer-modified α-hemolysin pores to alter the properties of this channel[72] and fluorescently labeled starburst dendrimers were exploited for nuclear pore sizing. More recently, dendrimers, among the other polyvalent compounds, were tested for their ability to block *E. coli* E69 pore-forming Wza K30 capsular polysaccharide transporter (see the suppl. material in ref 73). In the present study, we investigated the effects of cationic poly(amido amine) (PAMAM) dendrimers (Supporting Information, Figure S1B) on the PA_{63} and C2IIa pores in vitro and in cell-based experiments.

EXPERIMENTAL SECTION

Reagents. Minimum essential medium (MEM) and fetal calf serum were from Invitrogen (Karlsruhe, Germany) and cell culture materials from TPP (Trasadingen, Switzerland). Complete protease inhibitor, staurosporine and streptavidin-peroxidase were from Roche (Mannheim, Germany) and Page Ruler prestained Protein ladder from Fermentas (St. Leon Rot, Germany). Biotinylated NAD^+ was purchased from R&D Systems GmbH (Wiesbaden-Nordenstadt, Germany). Enhanced chemiluminescence (ECL) system was obtained from Millipore (Schwalbach, Germany) and nitrocellulose blotting membrane from Whatman (Dassel, Germany). Glutathione-agarose beads (Macherey-Nagel, Düren, Germany), benzamidine beads from GE Healthcare (Munich, Germany) and thrombin from Amersham Biosciences Europe GmbH (Freiburg, Germany). PA_{63} used in cell assays was kindly provided by Dr. R. John Collier, Department of Microbiology and Molecular Genetics, Harvard Medical School, Boston. For the bilayer lipid measurements, PA_{63} was purchased from List Biological Laboratories, Inc. (Campbell, CA, U.S.A.). The following chemical reagents were used: KCl, MES, KOH, and HCl (Sigma-Aldrich, U.S.A.), "purum" hexadecane (Fluka, Buchs, Switzerland), diphytanoylphosphatidylcholine, DPPC (Avanti Polar lipids, Inc., Alabaster, AL), pentane (Burdick and Jackson, Muskegon, MI), agarose (Bethesda Research Laboratory, Gaithersburg, MD). MQ water was used to prepare solutions. Primary amine (generations 1−4) and hydroxyl (generations 2 and 3) PAMAM dendrimers, commercially available at Dendritech Inc. (Midland, MI, U.S.A.) as w/w H_2O solutions, were a kind gift of Dr. Sergey Bezrukov and primary amine PAMAM dendrimers (generation 8 and 10) of Dr. Svetlana Glushakova (generations 8 and 10; both at NICHD, NIH, Bethesda, MD, U.S.A.). G0−G2 primary amino dendrons, mixed surface 75% OH/25% G2-NH_2 dendrimers, G0.5 carboxylate-Na terminated PAMAM dendrimers and G2 succinamic acid terminated PAMAM dendrimers were purchased from Dendritech, Inc. (Midland, MI, U.S.A.) as w/w water solutions. Generation 0 PAMAM dendrimer was purchased from Dendritech, Inc. (Midland, MI, U.S.A.) or synthesized by Dr. Ng (University of Ulm), as described below in detail.

Purification of Proteins. The recombinant proteins C2I, C2IIa, and C2IN-C3lim were purified as described previously.[74] The plasmid His-C2I-pET28 was kindly provided by Dr. M. R. Popoff (Institut Pasteur, Paris, France) and His-C2I expressed in *E. coli* BL21 and purified by affinity chromatography using TALON CellThru beads (Clontech Laboratories, Inc., Heidelberg, Germany). In brief, His-C2I was eluted with PBS containing 50 and 100 mM imidazole, fractions were pooled and buffer exchange and concentrating of protein was achieved with VivaSpin columns (Sartorius, Göttingen, Germany) according to the manufacturer's instructions.

Characterization of Dendrimers by Mass Spectrometry and NMR. All solvents and reagents were bought from commercial sources and used directly without further purification. Reactions were conducted under argon atmosphere and all solvents were distilled before use unless otherwise stated. The extent of reaction was monitored by thin layer chromatography using Merck 60 F254 precoated silica on aluminum (Merck Millipore, Darmstadt, Germany) using appropriate stains (e.g., iodine). Flash column chromatography was carried out on Acros Organics silica gel (Fisher Scientific, Schwerte, Germany) 0.035−0.070 mm, 60 Å. The ^1H and ^{13}C NMR spectra were measured using a Bruker DRX 400 spectrometer (Bruker Daltonics, Bremen Germany) and the shifts were referenced to residual solvent shifts in the respective deuterated solvents. Mass spectra were acquired on a Bruker Daltonics Reflex III MALDI TOF (Bruker Daltonics, Bremen Germany) or Shimadzu LCMS 2020 (Shimadzu, Berlin, Germany).

Synthesis of Generation 0 PAMAM Dendrimer Methyl Ester. Ethylenediamine (2.0 g, 33.3 mmol) was dissolved in MeOH (2 mL)

Table 1. Inhibition of Transmembrane PA_{63} and C2IIa Current by the PAMAM Dendrimer G1−G10 Expressed as Experimental IC_{50} Values and $IC_{50} \times n$

				PA_{63}/PAMAM binding reaction		C2IIa/PAMAM binding reaction	
generation	measured diameter, Å, refs 77, 78	surface groups	surface NH_2 group number, n	IC_{50}[a]	$IC_{50} \times n$	IC_{50}[a]	$IC_{50} \times n$
PAMAM-NH_2 Dendrimers, *cis*-Side Addition							
0 (Dendritech)	15	NH_2	4	231 ± 53 nM	924 ± 212 nM	940 ± 175 nM	3.76 ± 0.7 μM
0 (Ng)	15	NH_2	4	128 ± 44 nM	512 ± 176 nM	574 ± 147 nM	2.3 ± 0.6 μM
1	22	NH_2	8	5.3 ± 2.6 nM	42 ± 21 nM	146 ± 46 nM	1.1 ± 0.4 μM
2	29	NH_2	16	7.15 ± 4.7 nM	114 ± 67 nM	105 ± 44 nM	1.7 ± 0.7 μM
3	36	NH_2	32	5.0 ± 1.4 nM	161 ± 45 nM	73 ± 32 nM	2.3 ± 1.0 μM
4	45	NH_2	64	2.4 ± 1.3 nM	167 + 83 nM	520 ± 297 nM	33.3 ± 19.0 μM
8	97	NH_2	1024	0.22 ± 0.08 nM	226 ± 82 nM	46 ± 22 nM	47.1 ± 22.5 μM
10	135	NH_2	4096	0.16 ± 0.07 nM	655 ± 267 nM	158 ± 64 nM	647 ± 265 μM
PAMAM-NH_2 Dendrimers, *trans*-Side Addition							
0 (Ng)	15	NH_2	4	16.5 ± 3.3 μM	66 ± 13.2 μM		
1	22	NH_2	8	4.6 ± 1.7 μM	36.8 ± 13.6 μM		
PAMAM Dendrimers with Uncharged or Negatively Charged Surface Groups							
0.5		COONa	8	>400 μM			
2		OH		142 ± 36 nM			
2		SA		>150 μM			
3		OH		44.9 ± 13.8 nM			
"Imperfect" PAMAM-NH_2 Dendrimers							
2		75% OH/25% NH_2	4 (ave)	122 ± 35 nM	488 ± 140 nM		
0 dendron		NH_2	2	26 ± 7 nM	52 ± 14 nM		
1 dendron		NH_2	4	4.9 ± 0.7 nM	19.6 ± 2.8 nM		
2 dendron		NH_2	8	4.2 ± 0.9 nM	33.6 ± 7.2 nM		

[a]All data were calculated as means from two or three separate experiments; the errors are standard deviations. 0.1 M KCl solutions at pH 6 were buffered by 5 mM MES. Recordings were taken at 20 mV applied voltage, which was the *cis*-side positive.

and added methyl acrylate (17.2 g, 200 mmol). The reaction was subsequently stirred for 24 h at room temperature. The solvents and excess methyl acrylate were evaporated under reduced pressure before purifying using column chromatography (5−10% MeOH/DCM). 92% yield. ^{1}H NMR (400 MHz, $CDCl_3$, 298 K) δ (ppm): 3.64 (s, 12H), 2.75−2.72 (t, 8H, J = 6 Hz), 2.46 (s, 4H), 2.43−2.39 (t, 8H, J = 8 Hz); ^{13}C NMR (100 MHz, $CDCl_3$, 298 K) δ (ppm): 172.9, 52.2, 51.5, 49.7, 32.6; ESI-MS: m/z $[M + H]^+$ = 405.50.

Synthesis of Generation 0 PAMAM−NH_2 Dendrimer. Generation 0 PAMAM dendrimer methyl ester (1.0 g, 24.8 mmol) was dissolved in MeOH (1 mL) and added ethylenediamine (29.8 g, 496 mmol). The reaction was stirred at room temperature for 5 days. The solvents and excess ethylenediamine were evaporated under reduced pressure to afford the product in quantitative yield. ^{1}H NMR (400 MHz, D_2O, 298 K) δ (ppm): 3.21−3.18 (t, 8H, J = 6 Hz), 2.78−2.75 (t, 8H, J = 6 Hz), 2.68−2.65 (t, 8H, J = 6 Hz), 2.56 (s, 4H), 2.41−2.38 (t, 8H, J = 6 Hz); ^{13}C NMR (100 MHz, D_2O, 298 K) δ (ppm): 175.0, 50.0, 49.1, 41.7, 39.7, 32.6; High resolution MALDI-TOF: m/z $[M + H]^+$ = 517.3933 (calculated), 517.3935 (found).

Channel Reconstitution into Planar Lipid Bilayers. To form solvent-free planar lipid bilayers with the lipid monolayer opposition technique,[75] we used a 5 mg/mL stock solution of diphytanoylphosphatidylcholine (DPPC) in pentane. Bilayer lipid membranes were formed on a 60 μm (for single-channel measurements) or 150 μm (for multichannel measurements) diameter aperture in the 15 μm thick Teflon film that separated the two compartments, as described in detail elsewhere.[14] The 0.01−1 M aqueous solutions of KCl were buffered at pH 6 (MES) at room temperature (23 ± 0.5 °C). Single channels were formed by adding 0.5 to 1 μL of 20 μg mL^{-1} solution of PA_{63}, or 0.2 to 0.5 μL of 48 ng mL^{-1} solution of C2IIa to the 1.5 mL aqueous phase on the *cis*-half of the bilayer chamber. For multichannel experiments, we applied ∼1−2 μL of 0.2 mg mL^{-1} stock PA_{63} or 1−2 μL of 48 μg mL^{-1} stock C2IIa to the *cis*-side of the membrane. Under this protocol, PA_{63} and C2IIa channel insertions were always directional as judged by channel conductance asymmetry in the applied transmembrane voltage. The electrical potential difference across the lipid bilayer was applied with a pair of Ag-AgCl electrodes in 2 M KCl, 1.5% agarose bridges. In most of the experiments, the PAMAM dendrimers were added to the *cis*-compartment of a bilayer chamber, which was the side of PA_{63} and C2IIa addition. The *cis*-compartment is believed to correspond to the endosome-facing cap side of the channels. In several experiments, activity of PAMAM G0 and G1 amino-terminated dendrimers added to the *trans*-side of membrane was also investigated. Multichannel measurements were performed at 20 mV and single-channel measurements at 20−100 mV. The applied potential is defined as positive if it is higher on the side of protein addition (*cis*-side).

Conductance measurements were done using an Axopatch 200B amplifier (Axon Instruments, Inc., Foster City, CA) in the voltage clamp mode. Signals were filtered by a low-pass 8-pole Butterworth filter (Model 9002, Frequency Devices, Inc., Haverhill, MA) at 15 Hz for multichannel and 15 kHz for single-channel systems and sampled with a frequency of 50 Hz and 50 kHz in the multi- and single-channel experiments, respectively. Amplitude, lifetime, and fluctuation analysis was performed with ClampFit 10.2 (Molecular Devices) and OriginPro 8.5 (OriginLab) software as well as with software developed in-house.

Cell Culture and Intoxication Assays. Vero (African green monkey kidney) cells and HeLa (human cervix carcinoma) cells were cultivated at 37 °C and 5% CO_2 in MEM containing 10% heat-inactivated fetal calf serum, 1.5 g/L sodium bicarbonate, 1 mM sodium-pyruvate, 2 mM L-glutamine and 0.1 mM nonessential amino acids, 100 U/mL penicillin, and 100 μg/mL streptomycin. Cells were trypsinized and reseeded three times per week for at most 15−20 times. For cytotoxicity experiments, cells seeded in culture dishes were incubated at 37 °C in medium with the respective toxin in the absence or presence of the dendrimers. After the indicated incubation periods, pictures from the cells were taken by using a Zeiss Axiovert 40CFl

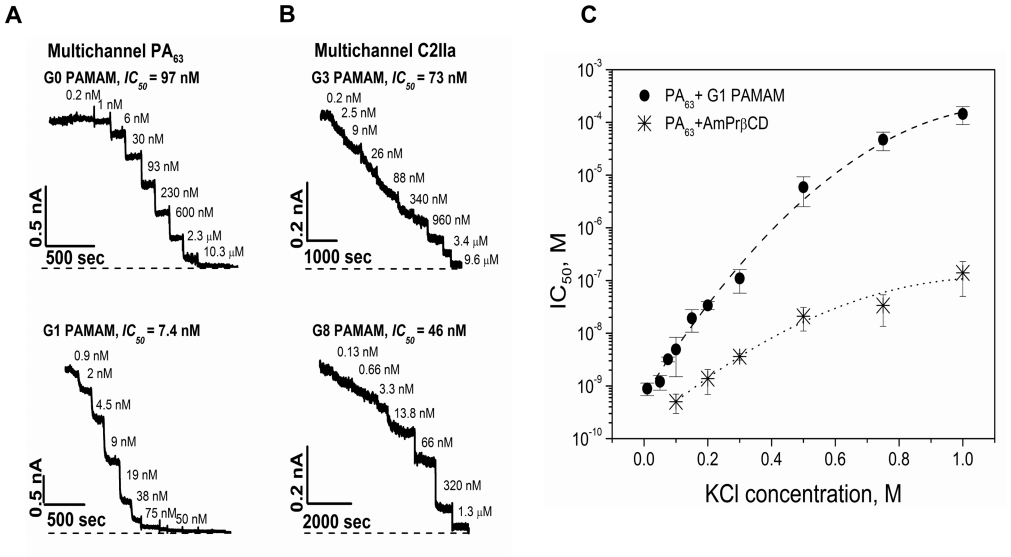

Figure 1. PAMAM Dendrimer-Induced PA_{63} and C2IIa Pore Inhibition at Multichannel Level. (A) Multichannel PA_{63} conductance changed by G0 (top) and G1 (bottom) dendrimer addition to the *cis*-compartment of bilayer chamber. (B) Multichannel C2IIa conductance changed by G3 (top) and G8 (bottom) dendrimer addition to the *cis*-compartment of bilayer chamber. The current recordings were additionally filtered over a 100 ms time interval. A 0.1 M KCl solutions at pH 6 were buffered by 5 mM MES. Recordings were taken at 20 mV applied voltage. The dashed lines represent zero current levels. The lowest and greatest dendrimer concentrations that are not marked in the figures are given in Figure S4 (titration curves). (C) IC_{50} values of the PA_{63}/G1-NH_2 binding reaction increase with KCl bulk concentration (filled circles). The salt dependence effect is stronger than the one reported earlier for the AmPrβCD blocker (stars).[14] The AmPrβCD data are reprinted with permission from ref 14. Copyright 2010 Elsevier.

microscope (Oberkochen, Germany) with a Jenoptik progress C10 CCD camera (Jena, Germany) to document the toxin-induced cell-rounding. To determine cytotoxic effects of the dendrimers, cells seeded in 96-well plates were incubated for up to 24 h with increasing concentration of dendrimers of the individual generations in the medium and cell rounding and cell viability were analyzed. Cell viability was measured with the CellTiter 96 AQ_{ueous} One Solution Cell Proliferation Assay (Promega, Mannheim, Germany) according to the manufacturer's instructions.

ADP-Ribosylation of Actin by C2I In Vitro. HeLa lysate (40 μg of protein) in 25 μL of ADP-ribosylation buffer (20 mM Tris-HCl (pH 7.5), 1 mM EDTA, 1 mM DTT, 5 mM $MgCl_2$, complete protease inhibitor) was incubated for 30 min at 37 °C in the presence or absence of 10 μM dendrimer. Then the lysate was treated with or without 10 ng/mL C2I and incubated for 15 min at 37 °C with 10 μM biotin-labeled NAD^+. The proteins were separated by SDS-PAGE according to the method of Laemmli, blotted onto a nitrocellulose membrane and the ADP-ribosylated (i.e., biotin-labeled) actin was detected by Western blotting with streptavidin-peroxidase and a subsequent chemiluminescence reaction using the ECL system according to the manufacturer's instructions. The intensity of the biotin-labeled actin was determined by densitometry using the Adobe Photoshop 7.0 software.

Analysis of Toxin-Binding to Cells. According to the recently described method,[76] HeLa cells were incubated for 30 min at 4 °C in serum-free medium with C2 toxin (800 ng/mL C2IIa + 400 ng/mL C2I) in the presence or absence of 10 μM dendrimer. As a control, cells were incubated with fresh serum-free medium. Then the medium was removed and cells were washed to remove any unbound toxin. A total of 25 μL of ADP-ribosylation buffer was added and cells were lysed. The lysate was incubated with 10 μM biotin-labeled NAD^+ for 30 min at 37 °C. The ADP-ribosylated (i.e., biotin-labeled) actin was detected by Western blotting exactly, as described before.

Reproducibility of the Experiments and Statistics. Each cell assay experiment was performed independently at least twice. Results from representative experiments are shown. Values ($n \geq 3$) are presented as means ± standard deviations (SD) using GraphPad Prism4 Software. Significance was determined by the Student's t test (***$p < 0.0005$; **$p < 0.005$; *$p < 0.05$). Planar lipid membrane measurements were repeated three times (G0-G10-NH_2 dendrimers, *cis*-addition, G2-OH, G3-OH, G2-SA dendrimers) or two times (G0-NH_2 and G1-NH_2 dendrimers, *trans*-addition, G0.5-COONa, G0-G2-NH_2 dendrons). Values are given as the means ± SD.

RESULTS

PAMAM Dendrimer Selection. The cationic PAMAM dendrimers, a well-characterized subclass of the multivalent dendrimers, are available as regularly branched highly monodispersed starburst polymers of different generations (G0−G10), which vary in size (d = 15−135 Å)[77,78] and surface charge (z = +4 to +4096). According to the manufacturer, each subsequent growth step represents a new "generation" of polymer with a larger molecular diameter, twice the number of reactive surface sites, and approximately double the molecular weight of the preceding generation. Since purity of the commercially available PAMAM dendrimers was previously shown to be questionable,[79,80] the G0−G3 dendrimers were characterized by mass spectrometry (not shown) and the respective NMR spectra are shown in Supporting Information, Figure S2A−E. These analytical measurements were also compared with data provided by Dendritech, Inc. on the originally supplied dendrimer products. To additionally verify quality of the supplied PAMAM dendrimers, G0-NH_2 dendrimer was synthesized in house (indicated in Table 1 as G0 (Ng)) with full characterization (Supporting Information, Figure S2A). The product was then compared with the commercially available G0 PAMAM dendrimer (indicated in Table 1 as G0 (Dendritech)) and used for the in vitro and cell assay studies. The initial choice of dendrimers was determined by the PA_{63} channel molecular models[81,82] and by the PA_{63} negative-stain electron microscopy image.[83] PA_{63} is an elongated ~170 Å mushroom-like pore. While the inner PA_{63} channel diameter is ~12−15 Å, the cap-side pore opening is approximately 4 times wider. Therefore, the PAMAM

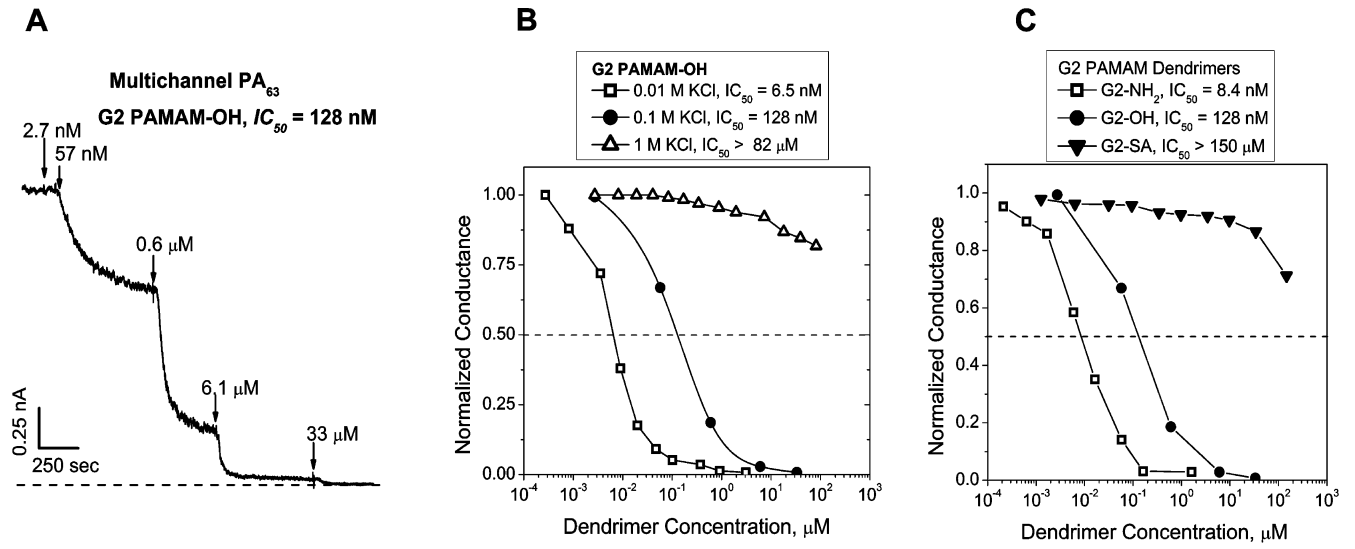

Figure 2. Influence of the PAMAM dendrimer surface groups on the PA_{63} ion current inhibition. (A) The PAMAM G2-OH dendrimer-induced PA_{63} inhibition at multichannel level. The current recordings were additionally filtered over 100 ms time interval. 0.1 M KCl solutions at pH 6 were buffered by 5 mM MES. Recordings were taken at 20 mV applied voltage. The dashed line represents zero current level. (B) Typical multichannel titration curves of the PAMAM−OH dendrimer-induced PA_{63} pore inhibition measured in 0.01 M (open squares), 0.1 M (filled circles), and 1 M KCl (open triangles) at 20 mV applied voltage. (C) Typical multichannel titration curves of the PA_{63} current inhibition by G2-NH_2 (open squares), G2-OH (filled circles), and G2-SA (filled triangles) PAMAM dendrimers. Recording were taken at 20 mV in 0.1 M KCl solutions at pH 6.

dendrimers G0−G4 ranging in their size from 15 to 45 Å are expected to be able to enter the pore, in contrast to the larger G5−G10 dendrimers. To test the potential inhibitory activity of higher generation dendrimers, we also chose to perform multichannel bilayer lipid measurements with 97 Å G8 and 135 Å G10 PAMAM dendrimers. Thus, as a first step, dendrimers of the generation G0, G1, G2, G3, G4, G8, and G10 were tested in the planar bilayer lipid membranes to compare their inhibitory activity toward PA_{63} and C2IIa pores in vitro. Because the dendrimers of generation 2 and higher exhibited effects on the morphology of the tested cells by their own, such as cell rounding within 3 h of incubation and decreased the amount of viable cells (Supporting Information, Figure S3), we focused on G0 and G1 in the cell-based experiments. Importantly, G0 and G1 dendrimers did not interfere with cell morphology or cell viability under such conditions (Supporting Information, Figure S3). Besides, because the PAMAM dendrimer G1 was identified as potential inhibitor against binary toxins both in cell-based experiments and in the planar bilayer membrane multichannel screening experiments and was not cytotoxic, we focused on this compound in the single-channel planar lipid bilayer studies, which aimed to determine mechanism of the pore/dendrimer binding reaction. Several PAMAM dendrimers functionalized with the uncharged hydroxyl and negatively charged carboxyl and succinamate surface groups instead of the positively charged amines were tested to explore the role of surface groups on the affinity of the blockers. We also tested channel-blocking activity of the so-called "imperfect" dendrimers, which included the G2 mixed surface 75% OH/25% NH_2 dendrimer and G0-G2-NH_2 dendrons.

Cationic PAMAM Dendrimer Blocks PA_{63} and C2IIa Channels in Planar Lipid Bilayers. We first compared PA_{63} and C2IIa channel blockage by the cationic PAMAM dendrimers over a range of generations using the planar lipid bilayer technique (Figure 1). All tested dendrimers inhibited PA_{63} and C2IIa channel conductance in a concentration-dependent manner when added to the *cis*-compartment of a bilayer chamber. Figure 1A,B show four representative recordings of the raw data titration curves in multichannel PA_{63} (Figure 1A) and C2IIa (Figure 1B) membranes modified by an increasing concentration of G0 (Figure 1A, top), G1 (Figure 1A, bottom), G3 (Figure 1B, top), and G8 (Figure 1B, bottom) PAMAM dendrimers.

When multivalent interactions are investigated, the macromolecule's avidity and affinity are frequently compared. In this study, we define affinity as strength of a single protein/functional group interaction and avidity (or functional affinity) as accumulated strength of multiple affinities of the multivalent dendrimers. To investigate the effect of the dendrimer charge on parameters of a blocker/pore binding reaction, we first experimentally determined the so-called 50% inhibitory concentration, IC_{50} of the PAMAM blockers and then calculated the half-maximal inhibitory concentration IC_{50} per-charge value. In many practical cases, IC_{50} values are used to analyze multichannel experiments. Therefore, IC_{50} corresponds to a dissociation constant, K_D, of a blocker/pore binding reaction when the relative reduction of ion current through a multichannel system due to the inhibitor addition is equal to 0.5. Table 1 summarizes both the experimental IC_{50} and calculated $IC_{50} \times n$ (shaded columns) values, where n is a number of the surface groups. $IC_{50} \times n$ represent the experimental IC_{50} values recalculated on the concentration of individual PAMAM amine branches.

Typical multichannel titration curves used to determine IC_{50} (Supporting Information, Figure S4) were calculated from the data similar to those shown in Figure 1A,B. We observed matching patterns in a dendrimer-induced current inhibition with both the PA_{63} and C2IIa multichannel membranes. In our system, the IC_{50} and $IC_{50} \times n$ values are in an inverse relationship with PAMAM avidity and affinity correspondingly. Thus, G1, G2, and G3 PAMAM dendrimers with the measured diameter of, correspondingly, 22, 29, and 36 Å and 8, 16, and 32 surface primary amines showed stronger binding affinity (lower $IC_{50} \times n$) when compared with the smaller low-

dx.doi.org/10.1021/bm500328v | Biomacromolecules 2014, 15, 2461−2474

generation, G0, and larger high-generation, G4, G8, and G10 PAMAM dendrimers (Supporting Information, Figure S5).

We found that binding parameters of the dendrimer/pore blocking reaction depend on a bathing electrolyte concentration suggesting strong involvement of electrostatic interactions into the pore/blocker binding reaction (Figure 1C). High salt concentrations reduce electrostatic forces significantly, most probably screening charges on both the dendrimer and the protein. This screening leads to a decrease in the dendrimer binding affinity by orders of magnitude. The observed effect was stronger compared to the one reported earlier for the more hydrophobic cationic cyclodextrins (Figure 1C, stars).

***cis*- versus *trans*-PAMAM Dendrimer Addition.** In the above experiments, we investigated the cationic dendrimer/pore binding reaction under conditions when the blockers were added only to the *cis*-side of the membrane. Because the PA_{63} and C2IIa channel insertion was shown to be unidirectional with the A component binding part of an oligomer facing the *cis*-side solution, we believe the *cis*-blocker application is physiologically relevant. Yet, we performed several experiments adding the G0-NH_2 and G1-NH_2 dendrimer blockers to the *trans*-side of the membrane (Supporting Information, Figure S6) and found that the compounds were active at the μM concentrations (Table 1). The *trans*-side pore blockage by the cationic G0 and G1 PAMAM dendrimers was, respectively, ~130 and 870 times weaker compared with the *cis*-side blockage under the constant 20 mV transmembrane voltage, which was *cis*-side positive. The sign of the voltage gradient in an acidified endosome membrane was reported to be inside-positive ($\varphi_{endosome} > \varphi_{cytosol}$) with $\Delta\varphi$ close to +(10−30) mV.[84−86] Therefore, the direction of the applied voltage gradient and its magnitude is within the physiologically relevant range.

PAMAM Dendrimers Terminated with Uncharged and Negatively Charged Groups Show Lower Channel-Blocking Activity. Interestingly, PAMAM dendrimers G2 and G3 functionalized with surface hydroxyl groups (PAMAM−OH) also inhibited PA_{63} channels in a concentration-dependent manner. However, the channel blocking activity of these compounds was significantly decreased compared with the PAMAM dendrimers carrying the positively charged surface amino groups (Table 1). Thus, we detected almost 20 times reduction in IC_{50} values between the PAMAM dendrimers G2 functionalized with the surface amino sites and those with the surface hydroxyl sites (Figure 2A). Note that we compared PAMAM G2-NH_2 and G2-OH dendrimers because G0-OH and G1-OH are not available commercially. We also tested G3-OH and observed 9 times decrease in avidity (higher IC_{50}) compared with G3-NH_2. This "residual" activity of the PAMAM−OH dendrimers could be determined by their net positive charge. Even though the surface charge of PAMAM−OH is equal to zero, the poly(amido amine) interior structure of PAMAM dendrimers holds a significant number of the tertiary amino groups that could be positively charged at subacidic pH.

To test this hypothesis, we investigated G2-OH activity in the KCl solutions of different concentrations (Figure 2B). Similar to the G1-NH_2 and AmPrβCD data (Figure 1C), the G2-OH's IC_{50} values were found to depend strongly on the bathing electrolyte concentrations, showing significant involvement of the electrostatic interactions between the negatively charged channel's lumen and the tertiary amino groups of G2-OH (Figure 2B). Moreover, when PAMAM dendrimers functionalized with negatively charged carboxyl and succinamate surface groups were added to the *cis*-side of the bilayer chamber, only a weak current decrease was recorded (Figure 2C, shown for G2-SA). Thus, with both 4-negatively charged half-generation G0.5 PAMAM dendrimer functionalized with carboxylate (PAMAM G2-COONa) and 16-negatively charged G2 PAMAM functionalized with succinamic acid (PAMAM G2-SA), 50% inhibitory constants were not reached at the dendrimer concentrations as high as 400 and 150 μM, correspondingly. The concentrations could not be increased further due to low concentrations of the manufactured stock dendrimer solutions.

Imperfect Cationic PAMAM Dendrimers Tested against the PA_{63} Pores. Activity of the amino PAMAM dendrimers was earlier shown to increase dramatically (>50-fold) when they were partially degraded at the amide linkage, which resulted in a heterodisperse population of compounds with different molecular weights.[87] The fractured dendrimers in complexes with DNA showed higher transfection levels when studied with cultured cells, which was explained by their lowered steric constrains (higher flexibility) compared with the intact PAMAM dendrimers. To test if this phenomenon is also relevant to the pore blockage, we investigated PA_{63} channel activity in presence of two different types of the "imperfect" PAMAM dendrimers (Supporting Information, Figure S7, Table 1). First, we used the mixed surface G2 75% OH/25% NH_2 PAMAM dendrimer, where the proportion of the positively charged primary amino groups was 25% on average (Figure S7A). Second, we investigated the pore binding activity of the G0, G1, and G2 dendrons (Figure S7B−D), which are the dendritic branches or the structurally incomplete dendrimers carrying respectively 2, 4, and 8 surface primary amines (chemical structures are shown in Figure S7E). The activity of G2 75% OH/25% NH_2 (122 ± 35 nM), which on average has two primary surface amines, was ~17× lower compared to its 16-positively charged G2-NH_2 analog (7.15 ± 4.7 nM). At the same time, activity of the G2-NH_2 dendron carrying 8 surface positive charges (IC_{50} = 4.2 ± 0.9 nM) was comparable with that of G1-NH_2 (IC_{50} = 5.3 ± 2.6 nM), which also has eight surface-positive charges. Besides, activity of the G1-NH_2 dendron functionalized with 4 positively charged groups was about 26× higher (IC_{50} = 4.9 ± 0.7) compared with that of the G-0 dendrimer, which also carries four positive charges (IC_{50} = 128 ± 44). The smallest G0 dendron, which has two surface primary amino groups also showed an impressive channel blocking activity with IC_{50} = 26 ± 7 nM. An increased pore-blocking activity of the low generation G0 and G1 dendrons could supposedly be explained by an increase in mobility of the surface primary amino groups, which had higher flexibility finding binding sites inside the pore. Moreover, a broken structure of the dendrons may allow a better access of the tertiary amino groups to the binding sites in channel lumen, increasing the effective charged of these "imperfect" compounds.

Two Modes of Dendrimer Action on the PA_{63} and C2IIa Channels. Quantitative analysis of the single-channel blockage proved difficult at the physiological salt concentrations because the residence time of the compound in the channel was very long. To obtain reliable statistics on the kinetic parameters of the binding reaction, we switched to 1 M KCl. This switch allowed us to more fully characterize and quantify this process on a single-channel level (Figure 3). Typical recordings of ion

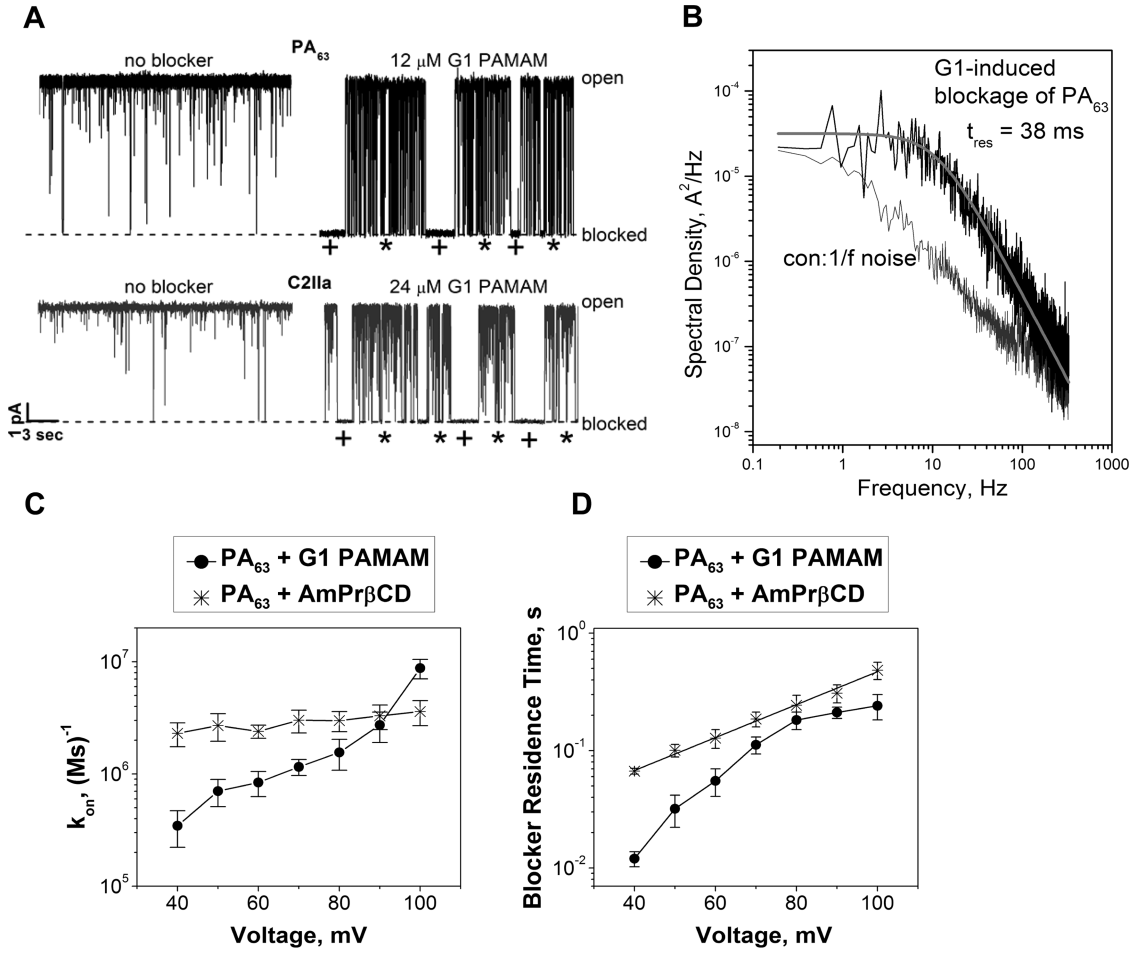

Figure 3. Single channel analysis of the PA_{63}/G1-NH_2 binding reaction. (A) Conductance of single PA_{63} (top) and C2IIa (bottom) channels in the absence (left) and presence (right) of PAMAM dendrimers G1 in the *cis*-side of the bilayer chamber shows the bimodal character of the dendrimer-induced action. Recordings are shown at 50 ms time resolution. 1 M KCl solutions at pH 6 were buffered by 5 mM MES. Recordings were taken at 50 mV applied voltage. Higher concentrations of G1 compared to the ones reported in Table 1 were needed because of the increased supporting electrolyte concentrations (1 M vs 0.1 M) used for the single-channel measurements. "*" and "+" indicate two different modes of the dendrimer binding. (B) Power spectral densities of PAMAM dendrimer G1 induced PA_{63} current fluctuations. PA_{63} single channel current fluctuations in presence of G1 (black spectrum) can be fitted by the single Lorentzian in contrast to $1/f$ noise in the blocker-free (con) solutions (shaded spectrum). (C, D) Kinetic parameters of PAMAM dendrimers G1 binding as functions of transmembrane voltage compared with the data earlier reported for AmPrβCD.[14] (C) The on-rate constant, k_{on}, of G1 binding to PA_{63} shows strong voltage dependence (filled circles) in contrast to the AmPrβCD blocker (stars). (D) The G1 binding time (filled circles) shows strong nonexponential voltage dependence in contrast to the AmPrβCD binding time (stars), which is nearly exponential (linear when plotted in a semi logarithmic scale). The AmPrβCD data are reprinted with permission from ref 14. Copyright 2010 Elsevier.

current through the single PA_{63} and C2IIa pores modified by PAMAM-NH_2 dendrimer G1 are shown in Figure 3A. Using single-channel analyses, we found that the inhibitive action of dendrimers is bimodal. First, cationic PAMAM dendrimers when added to the *cis*-side of the membrane (side of toxin addition) generate intense fluctuations in the current through a single channel (marked by "*") similar to those observed previously with the small-molecule[88] and cyclodextrin-based blockers.[6,15] These fluctuations are the fast transients between a fully open and blocked channel resulting from reversible binding of the cationic dendrimers to the residues inside the pores. Second, significantly longer voltage-dependent channel blockage events were also observed (Figure 3A, marked by "+"). The second mode of channel inhibition possessed the characteristic properties of a typical voltage-induced closed state of β-barrel channels. Earlier, similar two modes of the PA_{63} and C2IIa pore blockages were reported for the β-cyclodextrin-based cationic blockers.

To examine kinetic parameters of the dendrimer-induced blockage, we focused on a dendrimer binding reaction with the PA_{63} channel using current noise power spectrum analysis. Results for the G1 dendrimer-induced noise shown in Figure 3B demonstrate a good fit by a Lorentzian power spectrum at f < 300 Hz (smooth solid line through the experimental curve). The lower shaded spectrum represents PA_{63} $1/f$-like noise measured in blocker-free solution discussed earlier.[14] A single-Lorentzian shape of the power spectral density is associated with a two-state Markov process, where both the residence time in the blocker state and the channel lifetime in the open state are described by exponential distributions. The on- and off-rates of the blockage reaction were studied as functions of applied transmembrane voltage using G1/PA_{63} binding reaction (Figure 3C,D). Interestingly, in contrast to the cationic β-cyclodextrins (Figure 3C, stars), the k_{on}, increases as a function of voltage (Figure 3C), while the blocker residence time, t_{res}, being more voltage-dependent, demonstrates nonexponential

dx.doi.org/10.1021/bm500328v | Biomacromolecules 2014, 15, 2461−2474

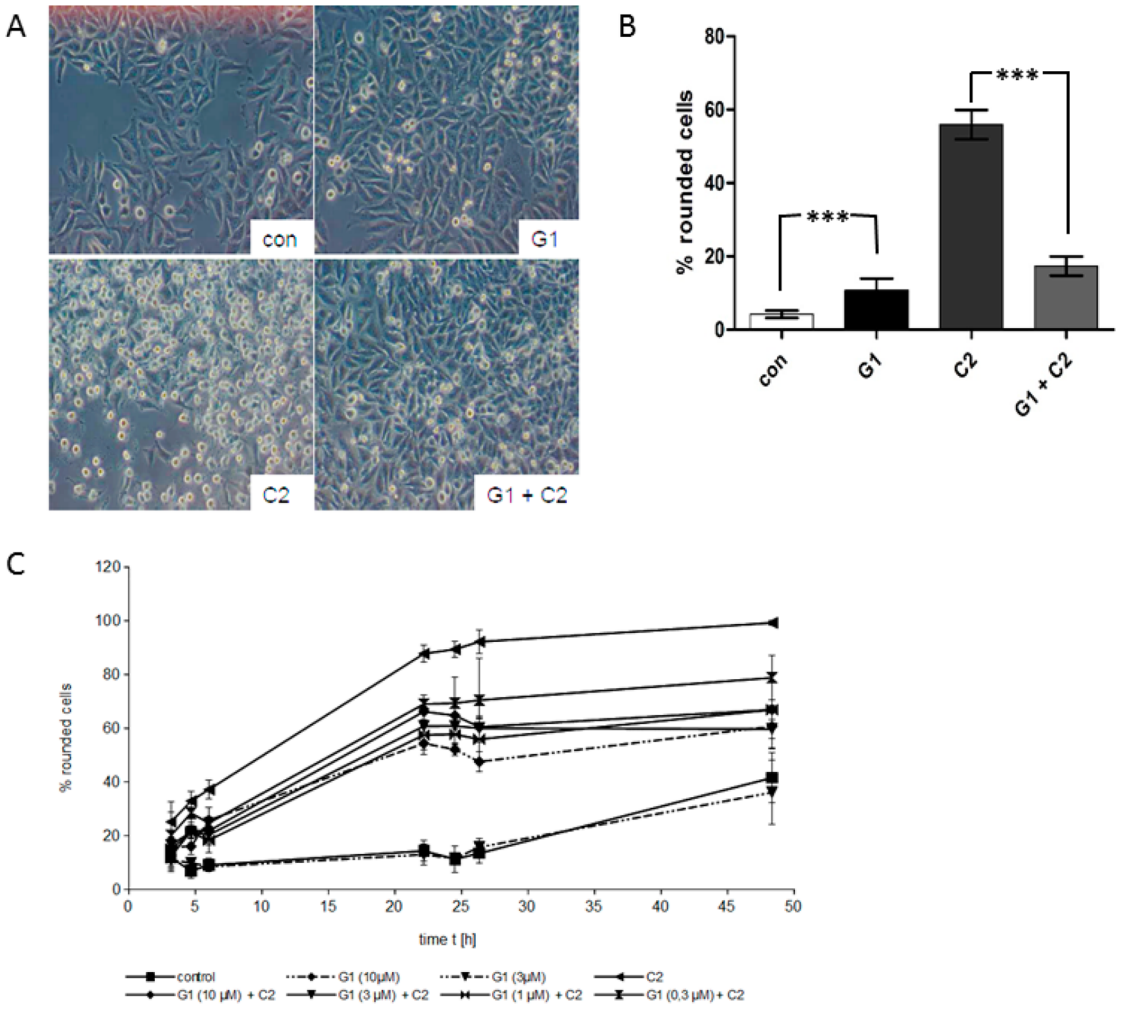

Figure 4. Effect of PAMAM dendrimer G1 on intoxication of HeLa cells with *C. botulinum* C2 toxin. HeLa cells were treated with C2 toxin (200 ng/mL C2IIa + 100 ng/mL C2I; 100 ng/mL C2IIa + 50 ng/mL C2I; 50 ng/mL C2IIa + 25 ng/mL C2I) in the presence of 10 μM final concentration of G1. For control (con), cells were left untreated (con) or treated with C2 toxin alone or with G1 alone. Pictures from the cells were taken after the indicated incubation periods. The number of total cells and round cells were counted from the pictures and the percentages of round cells calculated. (A) The morphology of cells and the calculated percentages of round cells are shown after 5.7 h treatment with C2 toxin (100 ng/mL C2IIa + 50 ng/mL C2I) and G1. Values are given as mean ± SD (n = 6) and significance was tested between toxin-treated samples with or without G1 and between untreated control cells and G1-treated cells, by using the Student's t test (***p < 0.0005). (B) Time-dependent inhibition of the intoxication of HeLa cells by C2 toxin. The values are given as mean ± SD (n = 6). (C) PAMAM dendrimer G1 protects cells from intoxication with C2 toxin in a time- and concentration-dependent manner. HeLa cells were incubated at 37 °C with 100 ng/mL C2I + 200 ng/mL C2IIa in the presence or absence of G1 (10, 3, 1, 0.3 μM). For control, cells were left untreated or treated with G1 (10 and 3 μM) alone. After the indicated incubation periods, pictures were taken to monitor the changes in cell morphology. The percentage of rounded cells was determined from the pictures. The values are given as mean ± SD (n = 6).

voltage dependence (Figure 3D). Single-channel behavior of the different PAMAM dendrimer types and generations is currently under investigation.

PAMAM Dendrimers from Generations 0 (G0) and 1 (G1) Protect Cells from Intoxication with C2 Toxin. First, we tested the effects of the PAMAM-dendrimers on HeLa cells. When cells were incubated with C2 toxin in the presence of G1 in the culture medium, less cells rounded up compared to treatment of cells with the C2 toxin alone, as shown in Figure 4A for a 5.7 h incubation period. Cell rounding is the consequence of the toxin-induced depolymerization of F-actin and therefore a specific parameter to monitor the cytotoxic mode of action of the actin-ADP-ribosylating toxins in the cytosol of cultured cells. A more detailed analysis with different concentrations of C2 toxin revealed a time-dependent delay of intoxication by 10 μM of G1 (Figure 4B). G1 alone had no relevant effects on cell morphology under these conditions (Figure 4B,C, Figure 8, and Supporting Information, Figure S3). Figure 4C shows the time- and concentration-dependent inhibitory effect of G1 on the intoxication of HeLa cells with C2 toxin over a 48 h incubation period. When PAMAM dendrimer G0 was used instead of G1, widely comparable results were obtained (Figure 5) however, the protective effect against C2 toxin was stronger in the case of G1.

Taken together, these results clearly demonstrate that PAMAM dendrimers G0 and G1 interfere with the mode of action of C2 toxin but give no hints on an underlying reason. However, the data indicate that 10 μM of G1 did neither inhibit the ADP-ribosylation of actin by C2I in vitro (Figure 6A), nor the binding of C2 toxin to its cell surface receptor (Figure 6B).

Moreover, G1 also protected cells from intoxication with C2IN-C3lim, a recombinant fusion toxin, which is delivered

dx.doi.org/10.1021/bm500328v | *Biomacromolecules* 2014, 15, 2461−2474

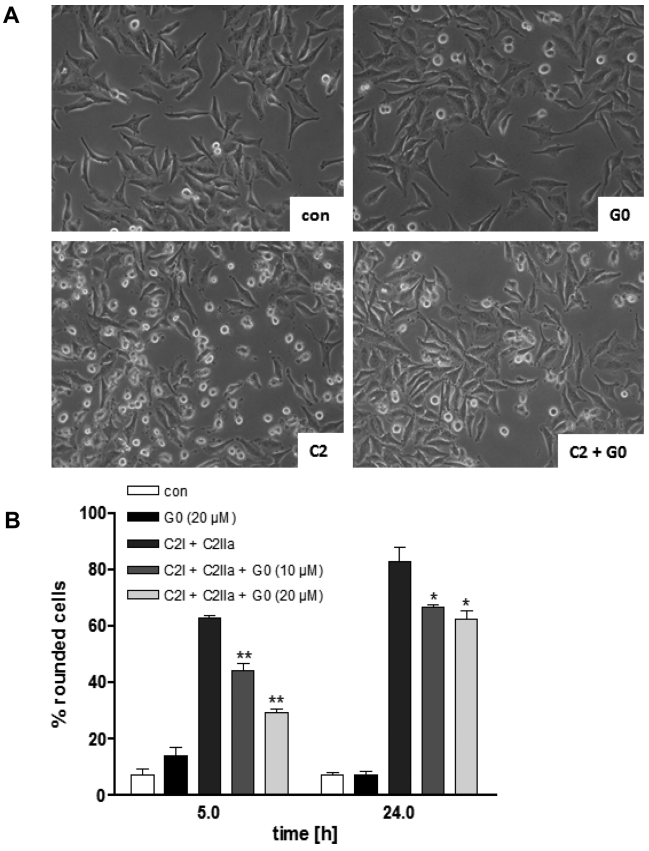

Figure 5. PAMAM dendrimer G0 protects cells from intoxication with C2 toxin. HeLa cells were incubated at 37 °C with 100 ng/mL His_6-C2I + 200 ng/mL C2IIa in the presence or absence of 10 μM and 20 μM G0. For control (con), cells were left untreated or treated with 20 μM G0 alone. Pictures were taken after 5 and 24 h. (A) The morphology of cells after 5 h of C2 toxin-treatment in the absence and presence of 20 μM G0 is shown. (B) The percentage of rounded cells was determined from the pictures. The values are given as mean ± SD (n = 3). Significance was determined by the Student's t test for cells treated with C2 toxin in the presence of G0 against cells treated with C2 toxin in the absence of G0 (**p < 0.005, *p < 0.05).

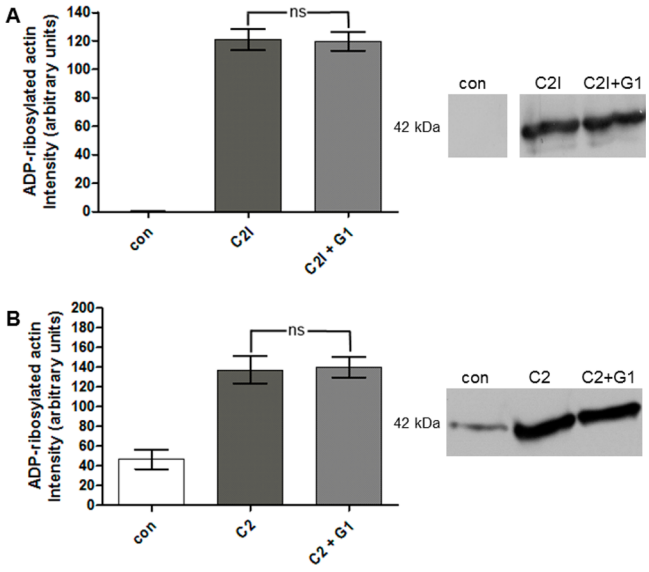

Figure 6. PAMAM dendrimer G1 does not affect enzyme activity and cell binding of C2 toxin. (A) PAMAM dendrimer G1 does not inhibit the ADP-ribosylation of actin by C2I in vitro. HeLa lysate (40 μg of protein in 25 μL) was incubated for 30 min at 37 °C in the presence or absence of G1. The lysate was treated with or without 10 ng/mL C2I and incubated for 15 min at 37 °C with 10 μM biotin-labeled NAD+. The proteins were separated by SDS-PAGE, blotted onto nitrocellulose and the ADP-ribosylated (i.e., biotin-labeled) actin was detected by Western blotting (right panel). The intensity of bands was determined by densitometry using the Adobe Photoshop 7.0 software (left panel). Values are given as mean ± SD (n = 3) and significance was tested between C2I-treated samples with or without G1 by using the Student's t test (ns = not significant). (B) PAMAM dendrimer G1 does not inhibit the receptor binding of C2 toxin. HeLa cells were incubated for 30 min at 4 °C in serum-free medium with C2 toxin (800 ng/mL C2IIa + 400 ng/mL C2I) in the presence or absence of 10 μM G1. As a control, cells were incubated with fresh serum-free medium. Then the medium was removed and cells were washed to remove any unbound toxin. After 25 μL of ADP-ribosylation buffer was added, cells were scraped of and lysed. ADP-ribosylation of actin was detected by Western blotting, as described in A.

into the cytosol by C2IIa (Supporting Information, Figure S8). C2IN is the enzymatic inactive domain of C2I, which interacts with C2IIa and mediates translocation of C2I- or C2IN-derived fusion proteins through C2IIa pores across endosomal membranes. This is a further indication that G1 interferes with the C2IIa-dependent protein transport into the cell. Thus, the dendrimers likely interfere with the C2IIa-mediated uptake of C2I during a later step of toxin internalization such as translocation from acidified endosomal vesicles into the host cell cytosol, which is plausible considering the fact that these substances inhibit the C2IIa translocation pores in vitro.

PAMAM-Dendrimers G0 and G1 Inhibit the PA_{63}-Mediated Delivery of His-C2I into the Host Cell Cytosol. Since G0 and G1 blocked the transmembrane pores formed by C2IIa and protective antigen (PA_{63}) in vitro and protected cells from intoxication with C2 toxin, we investigated whether these dendrimers also protect cells from intoxication with His_6-tagged C2I which is delivered into the cytosol by PA_{63}. Recently, it was demonstrated that His_6-tagged C2I translocates through PA_{63}-pores.[89] Most likely, positively charged His-residues at the N-terminus of C2I mediate the interaction with the pore and the translocation of C2I by mimicking positive charges in the N-terminal region of the lethal factor.[89] Therefore, this system might be the ideal model to compare the pore blocking effect of the dendrimers in a cell-based model since the same cargo protein, His-C2I, is delivered by two different translocation pores, C2IIa and PA_{63}, across endosomal membranes and allows the monitoring of the cytotoxic effects via C2I-mediated cell rounding. Having confirmed that G0 and G1 inhibit the intoxication of cells with C2IIa and His-C2I (Figure 5, Supporting Information, Figure S9), cells were challenged with PA_{63} + His-C2I in the absence and presence of G0 or G1. The results shown in Figures 7 and 8 indicate that both dendrimers delayed the intoxication of cells by PA_{63} + His-C2I as less cells rounded up in the presence of G0 or G1, suggesting that these dendrimers block the translocation pores formed by PA_{63} in the membranes of acidified endosomes in intact cells.

DISCUSSION

Discovery and characterization of multivalent therapeutic agents is a promising strategy in medicinal chemistry. This approach has already led to the design of several liposome-, polymer-, or cyclodextrin-based multivalent compounds specifically targeting different critical steps of the binary toxin's uptake.[1,6,11,12,90−94] Examples include multivalent inhibitors

dx.doi.org/10.1021/bm500328v | Biomacromolecules 2014, 15, 2461−2474

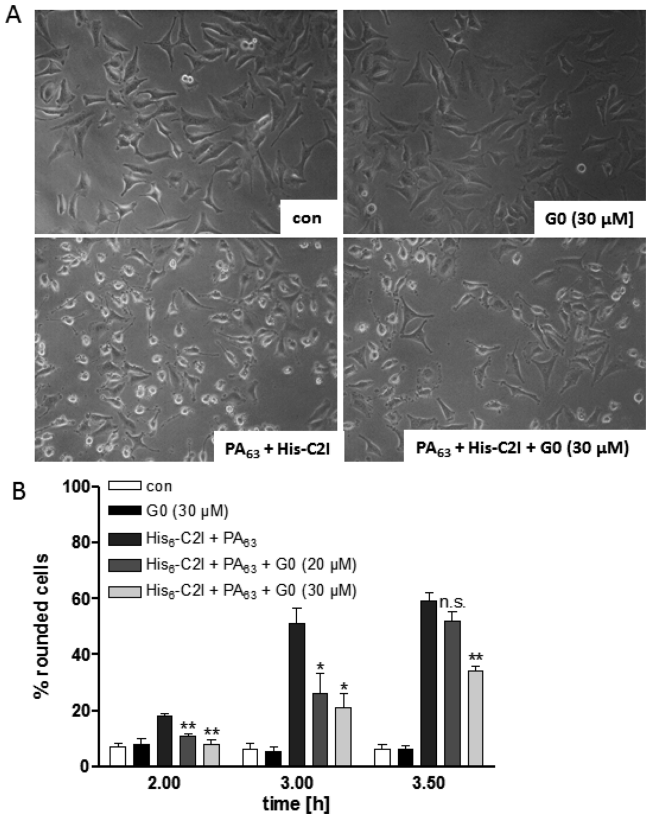

Figure 7. PAMAM dendrimer G0 protects cells from intoxication with His_6-C2I/PA_{63}. HeLa cells were incubated at 37 °C with 8 μg/mL His_6-C2I + 0.8 μg/mL PA_{63} in the presence or absence of 20 or 30 μM G0. For control (con), cells were left untreated or treated with G0 alone. After the indicated time points, pictures were taken to monitor the changes in cell morphology. (A) The morphology of cells after 3.5 h of toxin-treatment is shown. (B) The percentage of rounded cells was determined from the pictures. The values are given as mean ± SD (n = 3). Significance was determined by the Student's t test for cells treated with the toxin in the presence of G0 against cells treated with the toxin in the absence of G0 (***p < 0.0005; ** = p < 0.005, *p < 0.05).

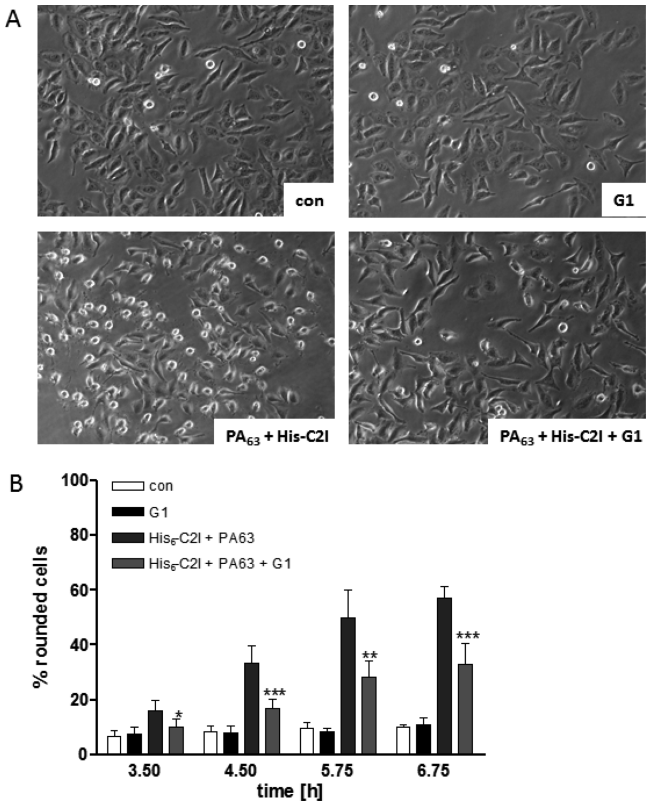

Figure 8. PAMAM dendrimer G1 protects cells from intoxication with His_6-C2I/PA_{63}. HeLa cells were incubated at 37 °C with 10 μg/mL His_6-C2I + 1 μg/mL PA_{63} in the presence or absence of 5 μM G1. For control (con), cells were left untreated or treated with G1 alone. After the indicated time points, pictures were taken to monitor the changes in cell morphology. (A) The morphology of cells after 4.5 h of toxin-treatment is shown. (B) The percentage of rounded cells was determined from the pictures. The values are given as mean ± SD (n = 6). Significance was determined by the Student's t test for cells treated with the toxin in the presence of G1 against cells treated with the toxin in the absence of G1 (***p < 0.0005; **p < 0.005; *p < 0.05).

targeting B-component binding to the cell surface receptors, inhibiting A-component interaction with the B-component oligomeric prepores, and obstructing channel-facilitated translocation of enzymatic A-components across the endosomal membrane. With all multivalent compounds, the reported half-maximum inhibitory concentrations per-functional group basis were significantly lower than those of monovalent compounds, indicating the significant enhancement of the activity of multivalent compounds. In the present study, we examined the antitoxin properties of positively charged PAMAM dendrimers, another group of multivalent compounds. Using a combination of in vitro and cell-based experiments, we showed that the cationic dendrimers inhibit channel-facilitated transport of the enzymatic components blocking ion-permeable PA_{63} and C2IIa. Remarkably, in vitro PA_{63} inhibitory concentrations of the commercially available PAMAM dendrimers (0.16−230 nM, depending on the generation) turned out to be comparable to the inhibitory concentrations of the first rationally designed cationic β-cyclodextrin-based blocker, AmPrβCD (0.55 nM),[14] which was selected out of dozens of related βCDs.[95] Therefore, the cationic dendrimers represent a group of potential lead compounds, suitable for further optimization and development as pore-blocking antitoxins.

The physical forces involved in the dendrimer/pore binding reaction require further investigation. Here we report that the inhibitory action of the PAMAM-NH_2 dendrimers is bimodal. The first inhibition mode is detected as reversible dendrimer binding to channel's lumen. Based on the strong dependence of the binding reaction equilibrium and kinetic parameters on solution concentration and transmembrane voltage (Figures 1C and 3C,D), we expect electrostatic interactions to prevail. One obvious way to increase activity of the dendrimers would involve a number of chemical modifications to create additional stabilizing short-range interactions between the channels and the blocker molecules. This approach was previously shown to be beneficial in the design of both small-molecule[54,61,63] and cyclodextrin-based[10,15,16] anthrax and C2 toxin inhibitors. Indeed, the blocking efficiency of the cationic compounds directly correlates with a number of aromatic groups in such small molecule or cyclodextrin-based blocker molecules, which was explained by their interaction with the PA_{63} and C2IIa's F427 and F428 ϕ-clamps.[16,54,58] Thus, it was demonstrated for such compounds that most of the attractive interactions responsible for the high binding strength of the compounds to their PA_{63} and C2IIa targets are due to the short-range forces

dx.doi.org/10.1021/bm500328v | Biomacromolecules 2014, 15, 2461−2474

other than Coulombic.[16] Introduction of these functional groups may also improve pharmacokinetic properties of the dendrimers,[96] such as resorption, plasma protein binding, and half-live time in the circulation, as well as biliary and renal excretion and ability to pass the transmembrane barrier. The second inhibition mode possesses many characteristic properties of the voltage gating observed with many β-barrel channels inserted into the planar bilayers. Besides, the G0-NH_2 and G1-NH_2 dendrimers were about 130 and 870 times more active when added from the *cis*-side of the membrane, which corresponds to the endosomal cap-side of the PA_{63} channel compared to the intracellular stem-side.

In this study, we also found that PAMAM G2 and G3 dendrimers functionalized with hydroxyl but not with carboxyl and succinamate surface groups inhibit PA_{63} channels in planar lipid bilayers in a concentration-dependent manner. The IC_{50} values for G2-OH and G3-OH were correspondingly 20 and 9 times lower than those determined for G2-NH_2 and G3-NH_2. Likewise with the amino terminated dendrimers, G2-OH-induced pore blockage was significantly weaker at high bathing electrolyte concentrations. We suggest that the "residual" activity of the PAMAM−OH dendrimers may originate from the positively charged tertiary amino groups at the branching points of the PAMAM core structure interacting with the negatively charged PA_{63} lumen. To that end, it is interesting to correlate the PAMAM pore-blocking activity with an effective charge density of the dendrimer molecules.[97−100] Indeed, counterion condensation induces a significant decrease in the nanoparticle effective surface charge density compared to its nominal or apparent geometric surface charge density.[97,101] The surface charge is often related to the zeta (ζ) potential, or the electrostatic potential at the electrical double layer surrounding a nanoparticle in solution. Nanoparticles with a ζ-potential between −10 and 10 mV are considered as neutral and nanoparticles with ζ-potentials greater than +30 mV or less than −30 mV as strongly cationic and strongly anionic, respectively.[102] A number of experimental studies exist where ζ-potential was obtained from measuring electrophoretic mobility of dendrimers using DLS. Thus, when measured in 10 mM NaCl, PAMAM G3-NH_2 had positive ζ-potential of +43.3 mV and PAMAM G3-OH was neutral (ζ-potentials = −5.8 mV). In addition, the ζ-potential in G3-G7 PAMAM dendrimer systems for various generations was calculated using several hundred nanosecond long fully atomistic molecular dynamics simulations.[103] For G3-NH_2, the ζ-potential ranged from ∼+22 to ∼+30 mV depending on the computation approach the authors used. Moreover, in contrast to the exponential behavior of the apparent geometric surface charge, the effective charge increases with dendrimer generation very slowly and saturates at high generations due to a strong accumulation of counterions. While these findings are instructional, the reported effective charge data should not be applied directly when the particle binding is investigated in confined geometries such as protein ion channels. The reason is that water molecules in ion channels exhibit structural and dynamic properties, which differ significantly from those found in bulk.[104] Thus, electrostatic environment of the channel lumen decreases mobility of water molecules, which was reported to result in significant reduction (down to 20) of the effective dielectric constant of water in the channel pore. Moreover, to enter the channel, the G0-G4 PAMAM dendrimers are expected to reorganize their solvation structure, losing all or almost all shell water molecules and counterions. These factors can alter considerably surface charge characteristics of the dendrimer molecules responsible for their interaction with the channel lumen.

It is important to address the potential translational issues that our approach might face. The method we used is based on search for a molecule that binds with high affinity to its target, preferably a universal one, such as the B-moiety of binary toxins. Conceptually, the drug design task is more complex and involves appropriate tuning of binding selectivity (avoidance of undesirable targets).[105] Indeed, even though dendrimers exhibit significantly lower toxicity than linear polymers,[106,107] the positively charged amino-terminated dendrimers are generally referred as less biocompatible compared to their neutral and negatively charged analogues.[108] In particular, dendrimers carrying $-NH_2$ surface groups displayed concentration- and generation-dependent toxicity and hemolysis with several cell lines.[106,108] Increased cytotoxicity of amino-terminated dendrimers may be explained by their interaction with the negatively charged cell surfaces, by hole formation, or by expanding holes at existing membrane defects.[109] Likewise, we had to limit our cell assay studies to G0 and G1 because the higher generation dendrimers were cytotoxic for the cell lines used. However, we have not detected any membrane instability over the used range of PAMAM concentrations with the planar bilayer measurements. At the same time, to remedy the cytotoxicity problem, numerous lead optimization studies are now focusing on the surface engineering approaches, which allow for masking the positive charges by a partial surface derivatization with chemically inert groups such as PEG or fatty acids[107] One of the most promising approaches involves encapsulation of dendrimers into poly(ethylene glycol)-*b*-poly(aspartic acid) micelles.[107] While stable at physiological conditions, these micelles disintegrate in the acidic environment of the endosome,[110,111] which, if attained, would allow positively charged dendrimers to be delivered directly to the binary toxin targets. In addition to the surface charge, the cytotoxicity of dendrimers was shown to depend on chemistry of the core.[108] For instance, the toxicity of positively charged cationic poly(propyleneimine) (PII) dendrimers was not generation-dependent.[106,112] Therefore, chemical modification of the dendrimer's core should be also explored. An increase in activity of the amino PAMAM dendrimers was also reached when the compounds were partially degraded to the so-called "fractured" or "imperfect" dendrimers.[87] Likewise, we observed nM-range channel blocking activity of the G0−G2-NH_2 dendrons with several compounds being somewhat more active that the intact dendrimers carrying equal number of the surface primary amines.

Here, we investigated multivalent cationic dendrimers, which is another group of pore blockers active against two different binary toxins: anthrax and C2. The common mechanism of protection against these toxins involves the blockage of the PA_{63} and C2IIa channel's lumen by the cationic compounds. Historically, the binding component of anthrax toxin, PA has been the key target in developing both preventive and therapeutic measures to combat anthrax. However, the PA-targeting approaches are believed to have certain limitations. For instance, in contrast to less stable PA, LF remains active in cells and in animal tissues for days, which is manifested in the continued cleavage of MEK proteins by the toxin during this time.[113] Moreover, PA was recently shown to translocate LF not only into the cytosol but also into the lumen of endosomal intraluminal vesicles that can later fuse and release LF into the cytosol.[114] At the same time, LF can survive in the vesicles for

days being fully protected from proteolytic degradation. Therefore, efficacy of the postexposure treatment with PA-targeting drugs can be time-dependent being more effective at the early stages of infection. A successful pharmacological therapy against the mode of action of binary bacterial toxins would probably include a combined and synergistic specific targeting of both the A and B components of the toxins.

CONCLUSIONS

To conclude, we report a fundamentally new application for PAMAM dendrimers as universal pore-blocking multivalent antitoxins. The cationic PAMAM dendrimers effectively block pore-mediated translocation of the A-components of two medically relevant binary bacterial toxins: anthrax toxin of *Bacillus anthracis* and C2 toxin from *Clostridium botulinum* both in vitro (nM range) and in cell-based assays (μM range). The ability of cationic dendrimers carrying multiple functional groups to effectively inhibit intracellular transport of enzymatic components illustrates the value of multivalent interaction in drug development. We believe the pore-blocking properties of these dendrimers should be explored in a rational design of inhibitors of other bacterial toxins where pore formation plays an important role in intracellular toxin transport across membranes or in perforating mammalian cell membranes to induce cell lysis.

ASSOCIATED CONTENT

Supporting Information

NMR characterization of G0-G3 dendrimers (Figure S2), four figures supporting the bilayer lipid membrane data and conclusions (Figures S4–S7), three figures supporting cell assay data and conclusions (Figures S2, S8, S9) and a graphical representation of the main idea of the study (Figure S1), which is also given as a Table of Contents graphic. This material is available free of charge via the Internet at http://pubs.acs.org.

AUTHOR INFORMATION

Corresponding Authors

*Phone: 202-319-6723. E-mail: nestorovich@cua.edu.

*Phone: 49-731-50065503. E-mail: holger.barth@uni-ulm.de.

Author Contributions

†These authors contributed equally (P.F. and F.B.).

Notes

The authors declare no competing financial interest.

ACKNOWLEDGMENTS

E.M.N. was supported by startup funds from The Catholic University of America. H.B. was financially supported by the Deutsche Forschungsgemeinschaft DFG (Grant BA 2087/2-2). We are very thankful to Dr. Michel R. Popoff (Institut Pasteur, Paris) for kindly providing plasmid His-C2I-pET28 to H.B., Dr. R. John Collier (Harvard Medical School, Boston) for providing PA_{63} used in cell-based assays, Dr. Sergey M. Bezrukov (NICHD, NIH) for G0-G4 PAMAM dendrimers, and Dr. Svetlana Glushakova (NICHD, NIH) for providing G8 and G10 PAMAM dendrimers. We thank Ulrike Binder for expert technical assistance and Dr. Sergey Bezrukov for fruitful discussion.

REFERENCES

(1) Vance, D.; Shah, M.; Joshi, A.; Kane, R. S. *Biotechnol. Bioeng.* **2008**, *101*, 429–434.

(2) Fasting, C.; Schalley, C. A.; Weber, M.; Seitz, O.; Hecht, S.; Koksch, B.; Dernedde, J.; Graf, C.; Knapp, E. W.; Haag, R. *Angew. Chem., Int. Ed.* **2012**, *51*, 10472–10498.

(3) Branson, T. R.; Turnbull, W. B. *Chem. Soc. Rev.* **2013**, *42*, 4613–4622.

(4) Mourez, M.; Kane, R. S.; Mogridge, J.; Metallo, S.; Deschatelets, P.; Sellman, B. R.; Whitesides, G. M.; Collier, R. J. *Nat. Biotechnol.* **2001**, *19*, 958–961.

(5) Gujraty, K.; Sadacharan, S.; Frost, M.; Poon, V.; Kane, R. S.; Mogridge, J. *Mol. Pharmaceutics* **2005**, *2*, 367–372.

(6) Karginov, V. A.; Nestorovich, E. M.; Moayeri, M.; Leppla, S. H.; Bezrukov, S. M. *Proc. Natl. Acad. Sci. U.S.A.* **2005**, *102*, 15075–15080.

(7) Basha, S.; Rai, P.; Poon, V.; Saraph, A.; Gujraty, K.; Go, M. Y.; Sadacharan, S.; Frost, M.; Mogridge, J.; Kane, R. S. *Proc. Natl. Acad. Sci. U.S.A.* **2006**, *103*, 13509–13513.

(8) Gujraty, K. V.; Joshi, A.; Saraph, A.; Poon, V.; Mogridge, J.; Kane, R. S. *Biomacromolecules* **2006**, *7*, 2082–2085.

(9) Joshi, A.; Saraph, A.; Poon, V.; Mogridge, J.; Kane, R. S. *Bioconjugate Chem.* **2006**, *17*, 1265–1269.

(10) Karginov, V. A.; Nestorovich, E. M.; Yohannes, A.; Robinson, T. M.; Fahmi, N. E.; Schmidtmann, F.; Hecht, S. M.; Bezrukov, S. M. *Antimicrob. Agents Chemother.* **2006**, *50*, 3740–3753.

(11) Rai, P.; Padala, C.; Poon, V.; Saraph, A.; Basha, S.; Kate, S.; Tao, K.; Mogridge, J.; Kane, R. S. *Nat. Biotechnol.* **2006**, *24*, 582–586.

(12) Rai, P. R.; Saraph, A.; Ashton, R.; Poon, V.; Mogridge, J.; Kane, R. S. *Angew. Chem., Int. Ed.* **2007**, *46*, 2207–2209.

(13) Moayeri, M.; Robinson, T. M.; Leppla, S. H.; Karginov, V. A. *Antimicrob. Agents Chemother.* **2008**, *52*, 2239–2241.

(14) Nestorovich, E. M.; Karginov, V. A.; Berezhkovskii, A. M.; Bezrukov, S. M. *Biophys. J.* **2010**, *99*, 134–143.

(15) Nestorovich, E. M.; Karginov, V. A.; Popoff, M. R.; Bezrukov, S. M.; Barth, H. *PLoS One* **2011**, *6*, e23927.

(16) Bezrukov, S. M.; Liu, X.; Karginov, V. A.; Wein, A. N.; Leppla, S. H.; Popoff, M. R.; Barth, H.; Nestorovich, E. M. *Biophys. J.* **2012**, *103*, 1208–1217.

(17) Karginov, V. A.; Nestorovich, E. M.; Schmidtmann, F.; Robinson, T. M.; Yohannes, A.; Fahmi, N. E.; Bezrukov, S. M.; Hecht, S. M. *Bioorg. Med. Chem.* **2007**, *15*, 5424–5431.

(18) Ragle, B. E.; Karginov, V. A.; Bubeck Wardenburg, J. *Antimicrob. Agents Chemother.* **2010**, *54*, 298–304.

(19) El-Hawiet, A.; Kitova, E. N.; Kitov, P. I.; Eugenio, L.; Ng, K. K.; Mulvey, G. L.; Dingle, T. C.; Szpacenko, A.; Armstrong, G. D.; Klassen, J. S. *Glycobiology* **2011**, *21*, 1217–1227.

(20) Polizzotti, B. D.; Maheshwari, R.; Vinkenborg, J.; Kiick, K. L. *Macromolecules* **2007**, *40*, 7103–7110.

(21) Polyzos, A.; Alderton, M. R.; Dawson, R. M.; Hartley, P. G. *Bioconjugate Chem.* **2007**, *18*, 1442–1449.

(22) Polizzotti, B. D.; Kiick, K. L. *Biomacromolecules* **2006**, *7*, 483–490.

(23) Sisu, C.; Baron, A. J.; Branderhorst, H. M.; Connell, S. D.; Weijers, C. A.; de Vries, R.; Hayes, E. D.; Pukin, A. V.; Gilbert, M.; Pieters, R. J.; Zuilhof, H.; Visser, G. M.; Turnbull, W. B. *ChemBioChem* **2009**, *10*, 329–337.

(24) Merritt, E. A.; Zhang, Z.; Pickens, J. C.; Ahn, M.; Hol, W. G.; Fan, E. *J. Am. Chem. Soc.* **2002**, *124*, 8818–8824.

(25) Fan, E.; O'Neal, C. J.; Mitchell, D. D.; Robien, M. A.; Zhang, Z.; Pickens, J. C.; Tan, X. J.; Korotkov, K.; Roach, C.; Krumm, B.; Verlinde, C. L.; Merritt, E. A.; Hol, W. G. *Int. J. Med. Microbiol.* **2004**, *294*, 217–223.

(26) Laventie, B. J.; Potrich, C.; Atmanene, C.; Saleh, M.; Joubert, O.; Viero, G.; Bachmeyer, C.; Antonini, V.; Mancini, I.; Cianferani-Sanglier, S.; Keller, D.; Colin, D. A.; Bourcier, T.; Anderluh, G.; van Dorsselaer, A.; Dalla Serra, M.; Prevost, G. *Biochem. J.* **2013**, *450*, 559–571.

(27) Kitov, P. I.; Lipinski, T.; Paszkiewicz, E.; Solomon, D.; Sadowska, J. M.; Grant, G. A.; Mulvey, G. L.; Kitova, E. N.; Klassen, J. S.; Armstrong, G. D.; Bundle, D. R. *Angew. Chem., Int. Ed.* **2008**, *47*, 672–676.

(28) Kitov, P. I.; Mulvey, G. L.; Griener, T. P.; Lipinski, T.; Solomon, D.; Paszkiewicz, E.; Jacobson, J. M.; Sadowska, J. M.; Suzuki, M.; Yamamura, K.; Armstrong, G. D.; Bundle, D. R. *Proc. Natl. Acad. Sci. U.S.A.* **2008**, *105*, 16837−16842.
(29) Kitov, P. I.; Sadowska, J. M.; Mulvey, G.; Armstrong, G. D.; Ling, H.; Pannu, N. S.; Read, R. J.; Bundle, D. R. *Nature* **2000**, *403*, 669−672.
(30) Gargano, J. M.; Ngo, T.; Kim, J. Y.; Acheson, D. W.; Lees, W. J. *J. Am. Chem. Soc.* **2001**, *123*, 12909−12910.
(31) Mulvey, G. L.; Marcato, P.; Kitov, P. I.; Sadowska, J.; Bundle, D. R.; Armstrong, G. D. *J. Infect. Dis.* **2003**, *187*, 640−649.
(32) Solomon, D.; Kitov, P. I.; Paszkiewicz, E.; Grant, G. A.; Sadowska, J. M.; Bundle, D. R. *Org. Lett.* **2005**, *7*, 4369−4372.
(33) Dawson, R. M.; Alderton, M. R.; Wells, D.; Hartley, P. G. *J. Appl. Toxicol.* **2006**, *26*, 247−252.
(34) Nestorovich, E. M.; Bezrukov, S. M. *Chem. Rev.* **2012**, *112*, 6388−6430.
(35) Barth, H.; Aktories, K.; Popoff, M. R.; Stiles, B. G. *Microbiol. Mol. Biol. Rev.* **2004**, *68*, 373−402.
(36) Collier, R. J. *Mol. Aspects Med.* **2009**, *30*, 413−422.
(37) Duesbery, N. S.; Webb, C. P.; Leppla, S. H.; Gordon, V. M.; Klimpel, K. R.; Copeland, T. D.; Ahn, N. G.; Oskarsson, M. K.; Fukasawa, K.; Paull, K. D.; Vande Woude, G. F. *Science* **1998**, *280*, 734−737.
(38) Vitale, G.; Bernardi, L.; Napolitani, G.; Mock, M.; Montecucco, C. *Biochem. J.* **2000**, *352* (Pt 3), 739−745.
(39) Levinsohn, J. L.; Newman, Z. L.; Hellmich, K. A.; Fattah, R.; Getz, M. A.; Liu, S.; Sastalla, I.; Leppla, S. H.; Moayeri, M. *PLoS Pathog.* **2012**, *8*, e1002638.
(40) Leppla, S. H. *Proc. Natl. Acad. Sci. U.S.A.* **1982**, *79*, 3162−3166.
(41) Dumetz, F.; Jouvion, G.; Khun, H.; Glomski, I. J.; Corre, J. P.; Rougeaux, C.; Tang, W. J.; Mock, M.; Huerre, M.; Goossens, P. L. *Am. J. Pathol.* **2011**, *178*, 2523−2535.
(42) Liu, S.; Zhang, Y.; Moayeri, M.; Liu, J.; Crown, D.; Fattah, R. J.; Wein, A. N.; Yu, Z. X.; Finkel, T.; Leppla, S. H. *Nature* **2013**, *501*, 63−68.
(43) Ohishi, I.; Odagiri, Y. *Infect. Immun.* **1984**, *43*, 54−58.
(44) Aktories, K.; Barmann, M.; Ohishi, I.; Tsuyama, S.; Jakobs, K. H.; Habermann, E. *Nature* **1986**, *322*, 390−392.
(45) Heine, K.; Pust, S.; Enzenmuller, S.; Barth, H. *Infect. Immun.* **2008**, *76*, 4600−4608.
(46) Klimpel, K. R.; Molloy, S. S.; Thomas, G.; Leppla, S. H. *Proc. Natl. Acad. Sci. U.S.A.* **1992**, *89*, 10277−10281.
(47) Barth, H.; Blocker, D.; Behlke, J.; Bergsma-Schutter, W.; Brisson, A.; Benz, R.; Aktories, K. *J. Biol. Chem.* **2000**, *275*, 18704−18711.
(48) Kintzer, A. F.; Thoren, K. L.; Sterling, H. J.; Dong, K. C.; Feld, G. K.; Tang, I. I.; Zhang, T. T.; Williams, E. R.; Berger, J. M.; Krantz, B. A. *J. Mol. Biol.* **2009**, *392*, 614−629.
(49) Blaustein, R. O.; Koehler, T. M.; Collier, R. J.; Finkelstein, A. *Proc. Natl. Acad. Sci. U.S.A.* **1989**, *86*, 2209−2213.
(50) Schmid, A.; Benz, R.; Just, I.; Aktories, K. *J. Biol. Chem.* **1994**, *269*, 16706−16711.
(51) Bachmeyer, C.; Benz, R.; Barth, H.; Aktories, K.; Gilbert, M.; Popoff, M. R. *FASEB J.* **2001**, *15*, 1658−1660.
(52) Haug, G.; Wilde, C.; Leemhuis, J.; Meyer, D. K.; Aktories, K.; Barth, H. *Biochemistry* **2003**, *42*, 15284−15291.
(53) Krantz, B. A.; Trivedi, A. D.; Cunningham, K.; Christensen, K. A.; Collier, R. J. *J. Mol. Biol.* **2004**, *344*, 739−756.
(54) Krantz, B. A.; Melnyk, R. A.; Zhang, S.; Juris, S. J.; Lacy, D. B.; Wu, Z.; Finkelstein, A.; Collier, R. J. *Science* **2005**, *309*, 777−781.
(55) Krantz, B. A.; Finkelstein, A.; Collier, R. J. *J. Mol. Biol.* **2006**, *355*, 968−979.
(56) Melnyk, R. A.; Collier, R. J. *Proc. Natl. Acad. Sci. U.S.A.* **2006**, *103*, 9802−9807.
(57) Lang, A. E.; Neumeyer, T.; Sun, J.; Collier, R. J.; Benz, R.; Aktories, K. *Biochemistry* **2008**, *47*, 8406−8413.
(58) Neumeyer, T.; Schiffler, B.; Maier, E.; Lang, A. E.; Aktories, K.; Benz, R. *J. Biol. Chem.* **2008**, *283*, 3904−3914.
(59) Kronhardt, A.; Rolando, M.; Beitzinger, C.; Stefani, C.; Leuber, M.; Flatau, G.; Popoff, M. R.; Benz, R.; Lemichez, E. *PLoS One* **2011**, *6*, e23133.
(60) Orlik, F.; Schiffler, B.; Benz, R. *Biophys. J.* **2005**, *88*, 1715−1724.
(61) Beitzinger, C.; Bronnhuber, A.; Duscha, K.; Riedl, Z.; Huber-Lang, M.; Benz, R.; Hajos, G.; Barth, H. *PLoS One* **2013**, *8*, e66099.
(62) Bachmeyer, C.; Orlik, F.; Barth, H.; Aktories, K.; Benz, R. *J. Mol. Biol.* **2003**, *333*, 527−540.
(63) Bronnhuber, A.; Maier, E.; Riedl, Z.; Hajos, G.; Benz, R.; Barth, H. *Toxicology* **2014**, *316C*, 25−33.
(64) Vance, D.; Martin, J.; Patke, S.; Kane, R. S. *Adv. Drug Delivery Rev.* **2009**, *61*, 931−939.
(65) Yannakopoulou, K.; Jicsinszky, L.; Aggelidou, C.; Mourtzis, N.; Robinson, T. M.; Yohannes, A.; Nestorovich, E. M.; Bezrukov, S. M.; Karginov, V. A. *Antimicrob. Agents Chemother.* **2011**, *55*, 3594−3597.
(66) Diaz-Moscoso, A.; Mendez-Ardoy, A.; Ortega-Caballero, F.; Benito, J. M.; Ortiz Mellet, C.; Defaye, J.; Robinson, T. M.; Yohannes, A.; Karginov, V. A.; Garcia Fernandez, J. M. *ChemMedChem* **2011**, *6*, 181−192.
(67) Wijagkanalan, W.; Kawakami, S.; Hashida, M. *Pharm. Res.* **2011**, *28*, 1500−1519.
(68) Helms, B.; Meijer, E. W. *Science* **2006**, *313*, 929−930.
(69) Thompson, J. P.; Schengrund, C. L. *Glycoconjugate J.* **1997**, *14*, 837−845.
(70) Thompson, J. P.; Schengrund, C. L. *Biochem. Pharmacol.* **1998**, *56*, 591−597.
(71) Branderhorst, H. M.; Liskamp, R. M.; Visser, G. M.; Pieters, R. J. *Chem. Commun.* **2007**, *47*, 5043−5045.
(72) Martin, H.; Kinns, H.; Mitchell, N.; Astier, Y.; Madathil, R.; Howorka, S. *J. Am. Chem. Soc.* **2007**, *129*, 9640−9649.
(73) Kong, L.; Harrington, L.; Li, Q.; Cheley, S.; Davis, B. G.; Bayley, H. *Nat. Chem.* **2013**, *5*, 651−659.
(74) Barth, H.; Preiss, J. C.; Hofmann, F.; Aktories, K. *J. Biol. Chem.* **1998**, *273*, 29506−29511.
(75) Montal, M.; Mueller, P. *Proc. Natl. Acad. Sci. U.S.A.* **1972**, *69*, 3561−3566.
(76) Lang, A. E.; Ernst, K.; Lee, H.; Papatheodorou, P.; Schwan, C.; Barth, H.; Aktories, K. *Cell. Microbiol.* **2014**, *16*, 490−503.
(77) Prosa, T. J.; Bauer, B. J.; Amis, E. J.; Tomalia, D. A.; Scherrenberg, R. *J. Polym. Sci., Part B: Polym. Phys.* **1997**, *35*, 2913−2924.
(78) Jackson, C. L.; Chanzy, H. D.; Booy, F. P.; Drake, B. J.; Tomalia, D. A.; Bauer, B. J.; Amis, E. J. *Macromolecules* **1998**, *31*, 6259−6265.
(79) Mullen, D. G.; Desai, A.; van Dongen, M. A.; Barash, M.; Baker, J. R., Jr; Banaszak Holl, M. M. *Macromolecules* **2012**, *45*, 5316−5320.
(80) van Dongen, M. A.; Desai, A.; Orr, B. G.; Baker, J. R., Jr; Holl, M. M. *Polymer* **2013**, *54*, 4126−4133.
(81) Nguyen, T. L. *J. Biomol. Struct. Dyn.* **2004**, *22*, 253−265.
(82) Lee, K. I.; Jo, S.; Rui, H.; Egwolf, B.; Roux, B.; Pastor, R. W.; Im, W. *J. Comput. Chem.* **2012**, *33*, 331−339.
(83) Katayama, H.; Janowiak, B. E.; Brzozowski, M.; Juryck, J.; Falke, S.; Gogol, E. P.; Collier, R. J.; Fisher, M. T. *Nat. Struct. Mol. Biol.* **2008**, *15*, 754−760.
(84) Van Dyke, R. W.; Belcher, J. D. *Am. J. Physiol.* **1994**, *266*, C81−94.
(85) Rybak, S. L.; Lanni, F.; Murphy, R. F. *Biophys. J.* **1997**, *73*, 674−687.
(86) Sonawane, N. D.; Thiagarajah, J. R.; Verkman, A. S. *J. Biol. Chem.* **2002**, *277*, 5506−5513.
(87) Tang, M. X.; Redemann, C. T.; Szoka, F. C., Jr *Bioconjugate Chem.* **1996**, *7*, 703−714.
(88) Blaustein, R. O.; Lea, E. J.; Finkelstein, A. *J. Gen. Physiol.* **1990**, *96*, 921−942.
(89) Beitzinger, C.; Stefani, C.; Kronhardt, A.; Rolando, M.; Flatau, G.; Lemichez, E.; Benz, R. *PLoS One* **2012**, *7*, e46964.
(90) Joshi, A.; Vance, D.; Rai, P.; Thiyagarajan, A.; Kane, R. S. *Chem.—Eur. J.* **2008**, *14*, 7738−7747.

(91) Joshi, A.; Kate, S.; Poon, V.; Mondal, D.; Boggara, M. B.; Saraph, A.; Martin, J. T.; McAlpine, R.; Day, R.; Garcia, A. E.; Mogridge, J.; Kane, R. S. *Biomacromolecules* **2011**, *12*, 791−796.
(92) Kane, R. S. *AIChE J.* **2006**, *52*, 3638−3644.
(93) Rai, P.; Vance, D.; Poon, V.; Mogridge, J.; Kane, R. S. *Chem.—Eur. J.* **2008**, *14*, 7748−7751.
(94) Vance, D.; Martin, J.; Patke, S.; Kane, R. S. *Adv. Drug Delivery Rev.* **2009**, *61*, 931−939.
(95) Karginov, V. A.; Yohannes, A.; Robinson, T. M.; Fahmi, N. E.; Alibek, K.; Hecht, S. M. *Bioorg. Med. Chem.* **2006**, *14*, 33−40.
(96) Kaminskas, L. M.; Boyd, B. J.; Porter, C. J. *Nanomedicine* **2011**, *6*, 1063−1084.
(97) Huang, Q. R.; Dubin, P. L.; Moorefield, C. N.; Newkome, G. R. *J. Phys. Chem. B* **2000**, *104*, 898−904.
(98) Welch, C. F.; Hoagland, D. A. *Langmuir* **2003**, 1082−1088.
(99) Dobrovolskaia, M. A.; Patri, A. K.; Potter, T. M.; Rodriguez, J. C.; Hall, J. B.; McNeil, S. E. *Nanomedicine (London, U. K.)* **2012**, *7*, 245−256.
(100) Dobrovolskaia, M. A.; Patri, A. K.; Simak, J.; Hall, J. B.; Semberova, J.; De Paoli Lacerda, S. H.; McNeil, S. E. *Mol. Pharmaceutics* **2012**, *9*, 382−393.
(101) Böhme, U.; Klenge, A.; Hänel, B.; Scheler, U. *Polymers* **2011**, *3*, 812−819.
(102) Clogston, J. D.; Patri, A. K. *Methods Mol. Biol.* **2011**, *697*, 63−70.
(103) Maiti, P. K.; Messina, R. *Macromolecules* **2008**, *41*, 5002−5006.
(104) Aguilella-Arzo, M.; Andrio, A.; Aguilella, V. M.; Alcaraz, A. *Phys. Chem. Chem. Phys.* **2009**, *11*, 358−365.
(105) Huggins, D. J.; Sherman, W.; Tidor, B. *J. Med. Chem.* **2012**, *55*, 1424−1444.
(106) Lee, C. C.; MacKay, J. A.; Frechet, J. M.; Szoka, F. C. *Nat. Biotechnol.* **2005**, *23*, 1517−1526.
(107) Svenson, S.; Tomalia, D. A. *Adv. Drug Delivery Rev.* **2005**, *57*, 2106−2129.
(108) Duncan, R.; Izzo, L. *Adv. Drug Delivery Rev.* **2005**, *57*, 2215−2237.
(109) Hong, S.; Bielinska, A. U.; Mecke, A.; Keszler, B.; Beals, J. L.; Shi, X.; Balogh, L.; Orr, B. G.; Baker, J. R., Jr; Banaszak Holl, M. M. *Bioconjugate Chem.* **2004**, *15*, 774−782.
(110) Zhang, G. D.; Harada, A.; Nishiyama, N.; Jiang, D. L.; Koyama, H.; Aida, T.; Kataoka, K. *J. Controlled Release* **2003**, *93*, 141−150.
(111) Jang, W. D.; Nishiyama, N.; Zhang, G. D.; Harada, A.; Jiang, D. L.; Kawauchi, S.; Morimoto, Y.; Kikuchi, M.; Koyama, H.; Aida, T.; Kataoka, K. *Angew. Chem., Int. Ed.* **2005**, *44*, 419−423.
(112) Malik, N.; Wiwattanapatapee, R.; Klopsch, R.; Lorenz, K.; Frey, H.; Weener, J. W.; Meijer, E. W.; Paulus, W.; Duncan, R. *J. Controlled Release* **2000**, *65*, 133−148.
(113) Moayeri, M.; Crown, D.; Jiao, G. S.; Kim, S.; Johnson, A.; Leysath, C.; Leppla, S. H. *Antimicrob. Agents Chemother.* **2013**, *57*, 4139−4145.
(114) Abrami, L.; Brandi, L.; Moayeri, M.; Brown, M. J.; Krantz, B. A.; Leppla, S. H.; van der Goot, F. G. *Cell. Rep.* **2013**, *27*, 986−996.